TEM annealing study of normal grain growth in silver thin films

Rand Dannenberg[a,*], Eric Stach[b], Joanna R. Groza[c], Brian J. Dresser[c]

[a]*BOC Coating Technology, Fairfield, CA 94533, USA*
[b]*National Center for Electron Microscopy, Lawrence Berkeley Lab, Berkeley, CA, USA*
[c]*Chemical Engineering / Materials Science Department, U C Davis, Davis, USA*

Abstract

Normal grain growth in 80-nm-thick sputter-deposited Ag films was studied via in situ heating stage transmission electron microscopy. The as-deposited films with an initial grain size of 40–50 nm were held at a series of temperatures (one per specimen) below 250°C. A grain growth exponent $n = 3$ from the law $D^n - D_o^n = k(T)t$ was calculated by minimizing the deviation in the fitting function to the experimental data. An activation energy for grain growth of 0.53 eV (53 kJ/mol) is found, which is close to surface diffusion. These findings are consistent with our previous work on abnormal grain growth in Ag: that grain growth in thin film nanocrystalline silver is dominated by surface diffusion mass transport. © 2000 Elsevier Science B.V. All rights reserved.

Keywords: Grain boundary; Growth mechanism; Silver; Sputtering

1. Introduction

Nanograined materials frequently display grain size dependent electrical transport properties, optical properties, and mechanical properties. The fine grain size, sometimes described as morphological metastability, is associated with an inherently high driving force to reduce the total grain boundary energy or induce coarsening. It is important for this metastability to survive either the processing steps or throughout the product life. Many processing techniques involve some high-temperature exposure. This exposure may compromise the nanosized features of the final product. Powder consolidation is such a process in which the goal is to densify the nanocrystalline powders with minimal grain coarsening. Grain growth in thin films is critical for their reliability, e.g. influencing mean time to failure in interconnect lines where large grain sizes lead to bamboo structures which are resistant to electromigration failure, and in contrast, thin film optical coatings where light scattering (diffuse reflection and transmission) is minimal with a small grain size.

Thermal stability of nanocrystalline materials has been the subject of recent reviews [1,2]. Similar to conventional materials, the early stages of grain coarsening of nanocrystalline materials is described by an equation:

$$D^n - D_o^n = k(T)t \tag{1}$$

where D is the average grain diameter, D_o is the initial grain diameter, n is the grain growth exponent, k is a constant and t is time. The grain growth constant is exponentially dependent on temperature and proportional to the grain boundary mobility:

$$k(T) \propto e^{-Q/k_b T} \tag{2}$$

*Corresponding author. AFG Development Group, 1311 Clegg Street, Suite B, Petaluma, CA 94954, USA. Tel.: +1-707-792-9864.
E-mail address: rand.dannenberg@afg.com (R. Dannenberg).

where T is temperature, k_b is the Boltzmann constant, and Q is the activation energy for the mass transport mechanism.

Koch and coworkers summarized the n values for the isothermal grain growth of bulk nanocrystals and compared them to the values for conventional polycrystalline materials [1]. At low temperatures, n values are high or grain growth is slow, similar to regular materials. Such increased n values are rationalized by restricted grain boundary mobility, which is most commonly due to pore or solute effects. In nanocrystalline materials such as iron, Mallow and Koch found an average n value of 12 at low temperatures but the n value decreased with increasing temperatures in the same way as for the coarse grained materials [1]. In ZrO_2–3 mol% Y_2O_3 ceramics, n is larger than 4 at low temperatures and decreases to 3 at intermediate temperatures [3]. In other cases, constant n values were reported, e.g. $n = 4$ in grain growth during sintering of Al_2O_3 [4] and TiO_2 [5] or $n \approx 3$ in TiO_2 and yttria stabilized ZrO_2 [6,7].

Activation energies for grain coarsening are generally difficult to assess particularly when the n-exponent deviates from the ideal value of 2. Malow and Koch compiled the existing activation energy data for grain coarsening in consolidated nanosize metals, intermetallic compounds and ceramics [2]. In most cases, the activation energy is close to that of grain boundary diffusion, which is similar to large-grained materials. Some exceptions were found for elemental nanometals with activation energies equal to that of lattice diffusion [1]. Two apparent activation energy values were calculated in nanocrystalline Fe: a low value for low-temperature 1.25 eV (125 kJ/mol) and a high value 2.48 eV (248 kJ/mol) corresponding to high temperatures [1]. The latter value was close to that of volume diffusion in iron and is similar to the value found in coarse-grained iron. The low temperature value is less than that for grain boundary diffusion. A low activation energy value for grain coarsening in early sintering stages was also calculated by Thunissen et al. in ZrO_2–5.8 mol% Y_2O_3, although some uncertainty may be due to an uncertain n value [7]. Eastman also reports a low activation energy for grain growth 0.4–1.2 eV (83 ± 40 kJ/mol) in nano-TiO_2 [6].

In nanocrystalline copper and silver compacts, the activation energy for the grain growth was 0.8 eV (83 kJ/mol) for copper and 1 eV (100 kJ/mol) for silver [8]. Both values are close to grain boundary diffusion activation energies. In some other studies of nanocrystalline copper, reduced values of the activation energy have been reported at 0.3 eV (30 kJ/mol), over a factor of two lower than those for polycrystalline material [9]. This suggests different mass transport mechanisms may be operative for different grain sizes.

The present study is an in situ study of normal grain growth in nanocrystalline sputter deposited Ag films. In a previous paper by the authors, the activation energy for abnormal grain growth was concluded to be 0.273 eV (27 kJ/mol), and this was interpreted as a surface diffusion limited process due to thermal grooving [10]. The intent of the present work is to study normal grain growth in thin silver films and compare the activation energy of the normal grains to that of the abnormal grains of our previous work. We will use Eq. (1) because it applies to normal grain growth, has been applied to both film and bulk specimens, and because the literature involving this growth law is vast.

2. Experimental procedure

Silver films were sputter deposited onto amorphous silicon nitride transmission electron microscope (TEM) specimens with a viewable area of 470 μm^2. The process chamber was evacuated to a base pressure on the order of 10^{-6} torr. The process gas pressure was 3 mtorr of Ar. A power density of 2.8 kW/817 mm was used. The target-to-substrate distance was 10 cm. The film thickness was determined using a Dektak profilometer and sheet resistance measurements to be 80 nm.

The specimens were sputtered ex situ to the TEM. To minimize the interaction with sulfur and water after deposition, specimens were prepared on the morning of the experiment, and transported to the National Center for Electron Microscopy (NCEM) at Lawrence Berkeley National Laboratory (LBNL) for in situ TEM analysis, which is approximately a 1-h exposure to air. At NCEM the specimens were analyzed using a JEOL 200 CX in situ TEM using a LaB_6 filament operating at 200 keV. The heating stage was able to ramp up to any temperature below 1000°C in 60 s.

The TEM holder used in these experiments is a Model 652-Ta double-tilt heating holder from Gatan, Inc. In this design, the sample is placed in a miniature tantalum furnace that is heated resistively. The sample temperature is determined by a K-type platinum/platinum–13% rhodium thermocouple that is affixed to the outer body of the furnace heater, which is calibrated by the manufacturer. This is done by placing a thinned 3-mm disc of tantalum to which a separate thermocouple has been attached into the holder. The holder is then placed in vacuum, and correspondence between the two thermocouples is checked over the range of temperatures between 25°C and 1000°C. It has been shown using solid phase epitaxial regrowth of amorphous silicon that for temperatures between 450°C and 700°C, the thermocouple readings accurately represent the temperature in the thinned area of plan view silicon TEM samples to within approximately 10°C [11]. It is believed that the level of accuracy of the temperature calibration for the Si_3N_4 window samples used in these experiments is similar.

Four specimens, one for each temperature, were heated from room temperature up to temperatures of 125, 175, 200 and 250°C. At each of their respective temperatures, micrographs were taken at times of 5, 10, 15, 30 and 45 min. Different magnifications were used for clarity and sufficient number of grains used for clarity and to image a sufficient number of grains .

To ensure that the temperature recorded was actually the temperature of the specimen, two tests were done on the specimen stage. First, it was verified that the electron beam does not produce a localized overheating. The specimen was heated to 100°C for a sufficient hold time until the growth stopped and a fixed area was observed with the beam fully saturated. The beam was then quickly moved onto other areas not previously exposed, and held there. No further growth under the beam was observed. This was repeated with other specimens at all other temperatures. In a second method, an Ag film was surface oxidized over several weeks in air. The surface oxide blocks surface and/or grain boundary diffusion paths, and prevents the de-wetting of the film from the substrate until the melting point (961°C). The oxidation prevented grain growth until 400°C which is consistent with a doubling of the activation energy in slightly oxidized Ag [8]. The film de-wetted at an indicated temperature of 960°C with the beam fully saturated. Since the melting point should be dominated by the bulk of the film (un-oxidized silver), we may interpret this as the beam heating having negligible effect on the indicated melting point of the material. This establishes also that the thermometer is properly calibrated, and correctly indicates the specimen temperature.

Scion Image, a software package based on NIH Image for the Macintosh, was used to collect grain size data from scanned micrograph pictures. For each time and temperature, diameter data were derived from the grain size area values. The different magnifications used to take the micrographs allowed for a good statistical sample of greater than 100 grains analyzed per time and temperature. Obviously abnormal grains (very large, many-sided, and non-circular) were excluded from the analysis. Only roughly circular grains amid the large abnormal grains were counted.

3. Analysis and results

Fig. 1 shows the isothermal evolution of grain size is slow with no evidence of a plateau at 125°C (0.32 of the melting temperature, T_m), but becomes noticeable at temperatures above 175°C (0.36 T_m). At high temperatures, grain growth is fast at the short annealing times, then growth rate decreases sharply, with the diameter plateauing for long annealing times greater than 30 min. Fig. 2 shows the histograms for the normal grains for the first three data points at 250°C. The Ag films in
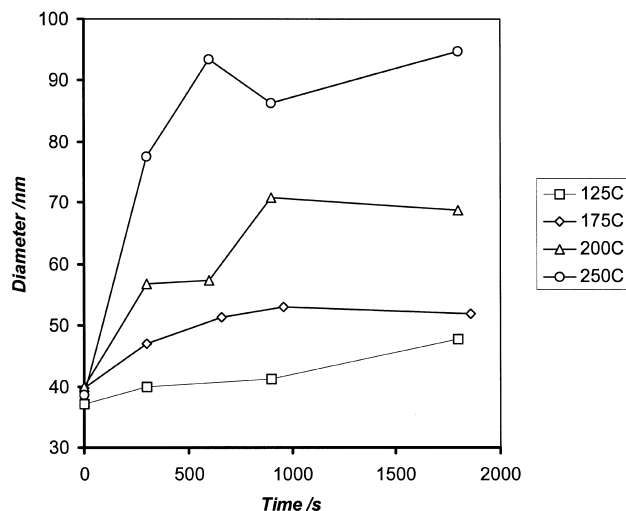

Fig. 1. Grain size as a function of time and temperature.

this study have microstructures similar to those published in Dannenberg et al. [10].

Using the isothermal annealing data, and excluding annealing durations greater than 30 min where the grain growth stagnates, $k(T)$ values were extracted from Eq. (1) for a particular n value. The k value was computed by linear least squares fit for each n and temperature. For a particular value of n, and for the resultant k at each temperature, E_{RMS}, the root mean square error was computed:

$$E_{RMS} = \frac{1}{N_H} \sum_T \frac{1}{N_T} \sum_i \left| D_{\exp_{i,T}} - D_{\mathrm{theory}_{i,T}} \right| \qquad (3)$$

where D_{theory} and $D_{\exp}$ are the theoretical grain diameters [from Eq. (1) for appropriate n and k] and experimental grain diameters, respectively, N_T is the number of data points analyzed at temperature T, N_H is the total number of hold temperatures investigated, and
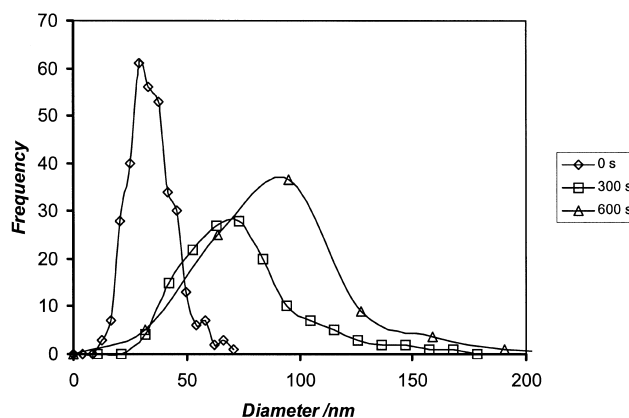

Fig. 2. Histograms for the normal grain of the first three data points for the 250°C anneal. The distributions are reasonably Gaussian with the mean nearly equal to the median.
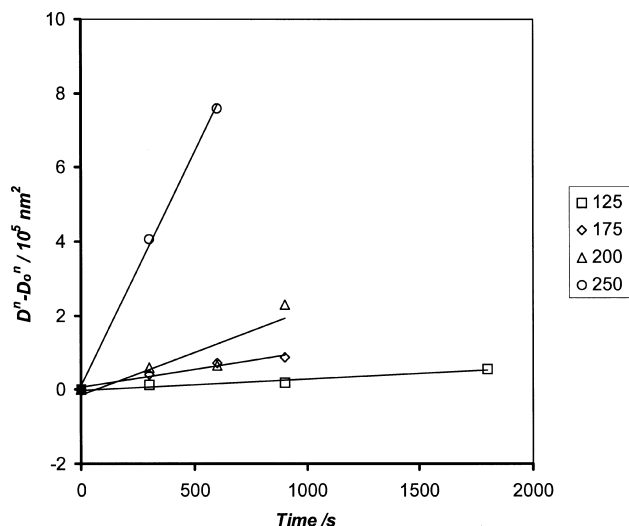
Fig. 3. Plot showing the method by which the respective data was fit to Eq. (1) with $n = 3$. We have not included data points in the flat regions of the D vs. t data.

Fig. 4. The root-mean-square error for the growth law given by Eq. (1) is minimized with $n = 3$.

the index i is the time index. This method of averaging removes the dependence on the number of data points, so E_{RMS} can be interpreted directly to be the average deviation between the fitting function and the data for all points, in nanometers. E_{RMS} was shown to be minimized for $n = 3$ (Figs. 3 and 4).

Each k value was then inserted into Eq. (2) with $n = 3$ and the corresponding temperature. The slope of $1/T$ vs. $\ln(k)$, determined by a linear least squares fit, yields an activation energy of 0.53 eV (53 kJ/mol) (Fig. 5).

4. Discussion

The value $n = 3$ is in close agreement with n values reported for pure nanocrystalline metals in the literature. For instance, Ganapathi et al. report a value of n between 2 and 4 for coarsening of nanocrystalline copper made by the sliding wear technique [9]. Huang et al. calculated $n = 1.85-1.92$ in nanocrystalline cop-
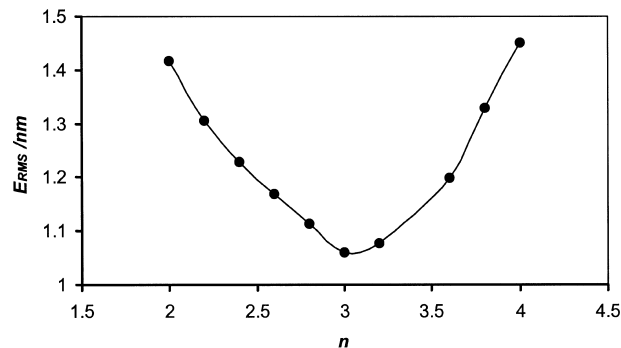
per by calorimetry [12]. This almost theoretical value may be rationalized by the high-temperature range of their grain-coarsening studies (between 0.3 and 0.75 T_m). As mentioned in the introduction, a similar value of $n \approx 3$ was found in TiO_2 and yttria stabilized ZrO_2 [6,7] The single value for n found at all temperatures used in the present study seems also reasonable since n is shown to generally increase above 0.45 T_m [1,2]. The maximum temperature used in these experiments is 0.42 T_m. The good fit of the data points (Fig. 3) is an additional indication that the value $n = 3$ does not change in the temperature range studied in this work. For verification, the activation energy for the classic value of $n = 2$ was calculated and found to be $Q = 0.453$ eV (45 kJ/mol) (Fig. 5). Furthermore, Q was calculated as a function of n in Fig. 6. It was found that values of n that greatly exceed the minimizing value of $n = 3$ are required to approach $Q = 0.95$ eV (95 kJ/mol), the activation energy for grain boundary diffusion in silver [13]. The fits of Eq. (1) (in plots analogous to Fig. 3) are very poor for these high values of n. The calculated activation energy for the normal grains, 0.53 eV (53 kJ/mol) for $n = 3$, is consistent with that measured for the abnormal grain growth, 0.274 eV (27 kJ/mol) in our previous paper, in that they are both significantly less than that of grain boundary diffusion in silver, 0.95 eV (95 kJ/mol) [10]. Both activation
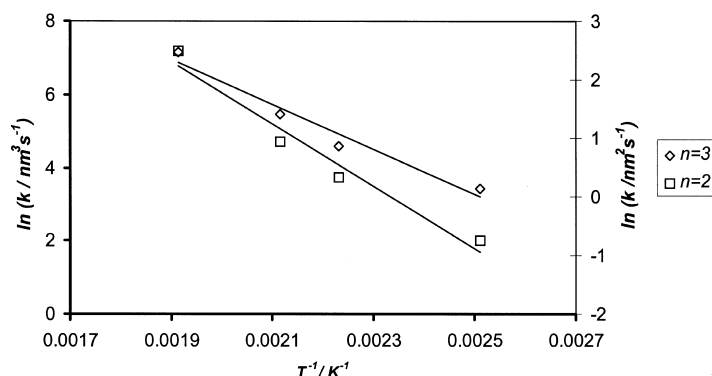

Fig. 5. The activation energy is computed from the slope of the solid lines. $Q = 0.53$ eV for the case of $n = 3$ and $Q = 0.453$ eV for $n = 2$.
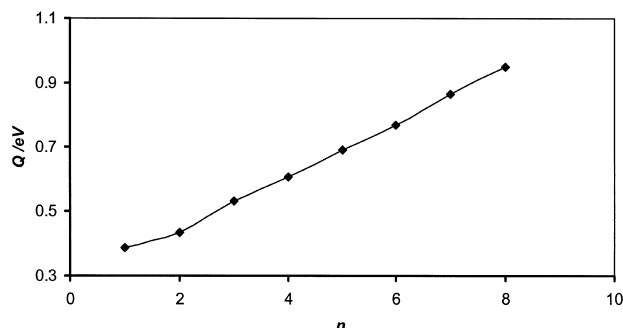
Fig. 6. Large values of *n*, which greatly exceed the error minimizing value of $n = 3$, are required to produce activation energies that approach those of grain boundary diffusion.

energies are consistent with a surface diffusion process, reported to be 0.3 eV (30 kJ/mol) in electromigration pore formation experiments [14].

The normal grain growth observed is consistent with theory. It is known that normal grain growth may occur when the grain size is less than the film thickness [15], and there are no opposing terms to curvature driven growth, such as grooving, precipitation drag, etc. In the present normal grain coarsening case, the initial grain size of the normal grains (40–50 nm) in the Ag films was approximately half of the film thickness (80 nm) and the final grain size was less than 100 nm (i.e. only 1.25 times film thickness) at the highest temperature studied (250°C). Therefore we do not believe that grooving effects were significantly damping normal growth in the time duration used for the analysis in the present work.

Abnormal grain growth may occur when the coarsening of some grains is suppressed or augmented by a variety of effects: (1) grain boundary grooving; (2) precipitate or impurity drag [16,17]; (3) substrate interactions causing the growth of a specific orientation (fiber texture) to be favored, typically a low-energy high-symmetry plane; and (4) statistical fluctuations and self shadowing effects during the deposition process that create a dilute concentration of randomly oriented grains, significantly larger than most, which grow by simple virtue that they have more than six sides. In our previous work on abnormal growth, we were able to fit the data to a growth law after Mullins with $n = 2$, where the driving force is proportional to the number of sides of the abnormal grains minus 6, $N_a - 6$ [10].

In our films, there is no indication of orientation dependence or texture. Electron diffraction ring patterns showed only continuous rings with no missing quadrants to imply texture, and a sampling of the largest abnormal grains showed single crystal diffraction patterns which are clearly not in-plane rotations, so a strong preferred orientation/fiber texture is unlikely. The method of monitoring ring pattern intensity changes of large area selected area diffraction patterns

during growth was not employed because of the unreliability of the method, stemming from the difficulty of measuring the relative intensity shifts from image processing artifacts.

Abnormal and normal grain growth was observed simultaneously in both the films of this study and our previous work, beginning at the lowest temperatures ~ 100°C [10]. In both cases, in the early stages of growth, the matrix of normal grains compete locally for growth according to a well-documented law, while the dilute abnormal grains consume the matrix grains, and stagnate due to thermal grooving. For long hold times, all grains stagnate indefinitely for the same hold temperatures.

5. Conclusions

The grain coarsening kinetics in nanocrystalline silver films was studied by in situ TEM heating. Both normal and abnormal grain growth occur simultaneously, with a matrix of normal grains competing locally according to a well-documented law $D^n - D_o^n = k(T)t$, and with a dilute concentration of abnormal grains having many more than six sides which consume the background matrix, eventually stagnating due to thermal grooving. Normal grain growth was studied up to $0.42\ T_m$. A value of $n = 3$ was found for the grain growth exponent. The activation energy calculated $Q = 0.53$ eV (53 kJ/mol) is close to that for the surface diffusion. This value is consistent with the result found for abnormal growth in which $Q = 0.273$ eV (27 kJ/mol), in that both activation energies are substantially lower than that reported for grain boundary diffusion, 0.95 eV (95 kJ/mol). We therefore conclude that grain growth in sputter deposited nanocrystalline Ag films, both normal and abnormal, is dominated by surface diffusion mass transport.

References

[1] T.R. Malow, C.C. Koch, Acta Mater. 45 (1997) 2177.
[2] T.R. Malow, C.C. Koch, in: D.L. Bourell (Ed.), Synthesis and Processing of Nanocrystalline Powder, TMS Powder Metallurgy, Warrendale, 1996, p. 33.

[3] M. Mayo, Int. Mater. Rev. 41 (1996) 85.

[4] J. Zhao, M.P. Harmer, Phil. Mag. Lett. 63 (1991) 7.

[5] H.G. Kim, K.T. Kim, Acta Mater. 47 (1999) 3561.

[6] J.A. Eastman, J. Appl. Phys. 75 (1994) 770.

[7] G.S.A.M. Thuenissen, A.J. Winnubst, A.J. Burggraaf, J. Eur. Ceram. Soc. 76 (1993) 319.

[8] B. Gunther, A. Kimpmann, H.D. Kunze, Scr. Metall. Mater. 27 (1992) 833.

[9] S.K. Ganapathi, D.M. Owen, A.H. Chockski, Scr. Metall. Mater. 25 (1991) 2699.

[10] R. Dannenberg, E. Stach, J.R. Groza, B.J. Dresser, Thin Solid Films 370 (2000) 54.

[11] E.A. Stach, R. Hull, J.C. Bean, K.S. Jones, A. Nejim, Microsc. Microanal. 4 (1998) 294.

[12] Y.K. Huang, A. Menovsky, F.R. deBoer, Nanostr. Mater. 2 (1993) 587.

[13] R.E. Hummel, H.J. Geier, Thin Solid Films 25 (1975) 335.[14]

[15] W.W. Mullins, J. Appl. Phys. 283 (1957) 333.

[16] J. Greiser, D. Muller, P. Mullner, C.V. Thompson, E. Arzt, Scr. Mater. 41 (7) (1999) 709.

[17] P.R. Rios, Acta Mater. 45 (1997) 1785.